学位論文　博士（医学）甲

Hyperthyroidism exacerbates ischemic reperfusion injury in the kidney

（過剰な甲状腺ホルモン補充は虚血再灌流下の尿細管上皮細胞のネクロトーシスの原因となる）

山口　安乃

山梨大学

Endocrine Journal

ORIGINAL

Advance Publication
doi:10.1507/endocrj.EJ21-0395

Hyperthyroidism exacerbates ischemic reperfusion injury in the kidney

Yasuno Yamaguchi[1)], Kohei Uchimura[1)], Kazuya Takahashi[1)], Toshihisa Ishii[1)], Shunichiro Hanai[2)] and Fumihiko Furuya[1)]

[1)] *Division of Nephrology, Department of Internal Medicine, Interdisciplinary Graduate School of Medicine and Engineering, University of Yamanashi, Yamanashi 409-3898, Japan*
[2)] *Division of Rheumatology, Department of Internal Medicine, Interdisciplinary Graduate School of Medicine and Engineering, University of Yamanashi, Yamanashi 409-3898, Japan*

Abstract. Thyroid hormones are critical regulators of vertebrate development and metabolism. Under hyperthyroid conditions, excess thyroid hormones induce expression of several enzymes and activities *via* activation of ligand-bound thyroid hormone receptors (TRs). Arginase (ARG) is downstream of a ligand-bound TR and overexpression of ARG2 induces the production of reactive oxygen species and subsequent exacerbation of kidney ischemia/reperfusion (I/R) injury. To clarify the association between I/R-induced kidney injury and hyperthyroidism, mice were pretreated with L-thyroxine (LT4) or vehicle alone, then subjected to I/R. Proximal tubular cell-specific conditional knockout of thyroid hormone receptor β (TRβcKO) mice was generated and the effects of I/R were analyzed. Hyperthyroidism enhanced tubular damage and fibrosis in the kidneys of mice after I/R. Hyperthyroidism induced tubular cell necroptosis following inflammatory cell accumulation in the kidney after I/R. ARG2 expressions and reactive oxygen species accumulated in the kidneys of hyperthyroid mice after I/R, but these changes were ameliorated in the kidneys of TRβcKO mice. Hyperthyroidism-enhanced kidney injury was ameliorated in the kidney of TRβcKO mice after I/R. These results suggest that excess thyroid hormones are disadvantageous for the kidney under ischemic stress. Overt hypothyroidism represents a severe thyroid hormone deficiency disease that requires LT4 treatment, while overreplacement or iatrogenic thyrotoxicosis might cause kidney injury.

Key words: Thyroid hormone receptor, Hyperthyroidism, Arginase, Kidney injury

THYROID HORMONES maintain cell viability *via* cell differentiation or proliferation. Thyroxine (T4) is converted to the active form, triiodothyronine (T3), which binds to thyroid hormone receptors (TRs) that function as ligand-dependent transcription factors to regulate the expression of target genes [1]. Two TR genes, THRA and THRB, encode 4 TR isoforms: α1, β1, β2, and β3. These isoforms are expressed in a tissue- or development-dependent manner. Under hyperthyroid conditions, excess thyroid hormone signal induces expression and activity of several enzymes. In hyperthyroid animals, enzymes such as arginase (ARG) for the L-arginine metabolic pathway are upregulated in the kidney, aorta, or heart [2]. Hypothyroidism is speculated to represent a factor associated with declining kidney function, but management of subclinical hypothyroidism with chronic kidney disease (CKD) remains controversial [3]. Hyperthyroid-induced kidney injury is largely caused by hemodynamic, metabolic, or cardiovascular disorders [3, 4], while recent reports have suggested that hyperthyroid-associated changes in L-arginine metabolism play important roles in kidney dysfunction [4, 5].

ARG is an enzyme that converts L-arginine into L-ornithine and urea. Two ARG isoforms are expressed in mammals: ARG1 and ARG2 [6]. ARG1 is mainly expressed in the liver and provides ammonia detoxification through the urea cycle. ARG2 is predominantly and constitutively expressed in the renal proximal tubular cells (PTCs) and regulates the production of nitric oxide (NO), because ARG2 competes with NO synthase (NOS) for the common substrate L-arginine. Indeed, upregulation of ARG2 expression and activity reduced the production of NO from L-arginine and NOS uncoupling induced the production of reactive oxygen species (ROS) instead of NO, following exacerbation of the kidney injury [6].

Submitted Jun. 25, 2021; Accepted Sep. 14, 2021 as EJ21-0395
Released online in J-STAGE as advance publication Oct. 9, 2021
Correspondence to: Fumihiko Furuya, Division of Nephrology, Department of Internal Medicine, Interdisciplinary Graduate School of Medicine and Engineering, University of Yamanashi, 1110 Shimokato, Chuo, Yamanashi 409-3898, Japan.
E-mail: ffuruya@yamanashi.ac.jp

Ischemia-reperfusion (I/R) injury is a pathological process that leads to acute kidney injury (AKI) and a subsequent repair process that restores the kidney to normal morphology and function if the injury is mild, or alternatively leads to permanent damage, interstitial fibrosis and CKD [7, 8]. The degree of renal ischemia and number of ischemic episodes are both associated with the severity and progression to CKD.

After I/R injury, ROS are excessively generated, causing severe damage inside tissues and inducing injuries *via* inflammatory responses [9]. Our research hypothesis was that thyroid dysfunction is associated with the development of interstitial inflammation and kidney injury. Herein, we focused on the L-arginine metabolic pathway after I/R injury under hyperthyroid conditions. We also explored whether inhibition of thyroid hormone signals would reduce renal injury using mice with specific conditional knockout of TRβ in PTCs. Our findings clarified the mechanisms underlying the deleterious effects of AKI and the excess thyroid hormone signaling pathway.

Materials and Methods

Animals

The animal experimental protocol was conducted in accordance with the guidelines of the "Animal Experiment Rules of the University of Yamanashi" established by the Animal Experimentation Facility at the University of Yamanashi. All procedures were approved by the Institutional Animal Care and Use Committee of the University of Yamanashi. Male C57BL/6 mice as wild-type controls were purchased from CLEA Japan (Tokyo, Japan).

To generate the TRβ floxed allele ($TR\beta^F$), we generated a targeting vector consisting of a 5' homologous sequence followed by a Pgk-neo cassette that is flanked by 2 flippase recognition target (Frt) sites. The targeted 1.3-kb region consists of exons 4 and 5 of *TRβ* flanked by 2 flox sites. We deleted the neo cassette by flippase-mediated recombination. N-myc downstream-regulated gene-1 (Ndrg1)$^{CreERT2/+}$ mice were provided by Professor Yanagita of Kyoto University [10]. Ndrg1, which is abundantly expressed in mature proximal tubules [11], drives tamoxifen (Tam)-inducible Cre recombinase (Cre^{ERT2}) and the Cre protein is expressed in all mature PTCs and is only activated after administration of Tam in Ndrg1$^{CreERT2/+}$ mice. $TR\beta^F$ mice were mated with Ndrg1$^{CreERT2/+}$ to generate $TR\beta^{F/F}$ Ndrg1$^{CreERT2/+}$ mice.

We administered mice with Tam at 150 mg/kg body weight (Merck, St. Louis, MO) by intraperitoneal injection for 5 consecutive days, to generate conditional-knockout mice with PTC-specific inhibition of TRβ expression (TRβcKO). Genotyping was performed by polymerase chain reaction (PCR) amplification of the tail DNA. Primers for $TR\beta^F$ were 5'-TGTTATTTTTAACCT GAGCCTTCTG-3' and 5'-AAGAATCCAAGTTCTGTT GACTGAG-3'.

Male C57BL/6 mice or TRβcKO mice were pretreated with oral administration of 250 μg/kg of L-thyroxine (LT4) (Merck) (hyperthyroid group) or vehicle (euthyroid group) for 14 days. Mice in each group were anesthetized and placed on a warming plate at a temperature of 37°C, and bilateral renal arteries were clamped for 45 min, followed by reperfusion under anesthesia. These mice were killed 14 days after this induction of I/R injury. Mice with sham operation were treated as controls.

Primary proximal tubular cell culture

The protocols for isolated PTCs for primary culture were as reported previously [12], with minor modifications to analyze the effects of hypoxia and thyroid hormone on PTCs. The renal cortex was minced in an ice-cold plate and digested for 15 min with 0.75 mg/mL of collagenase IV at 37°C in Hank's buffer. Digestion was stopped by mixing with 10% horse serum and washed twice with ice-cold Hank's buffer. PTCs were purified by 10 min of centrifugation at 2,000 × *g* in 32% Percoll and cultured in Dulbecco's modified Eagle's medium/F-12 medium containing 5% fetal bovine serum as regular serum (RS) or 5% resin-stripped fetal bovine serum as T3-depleted serum (TdS) [13, 14], then exposed to reagents under normoxia (21% O_2) or hypoxia (1% O_2), in an O_2-controllable *in vitro* incubator (Model-9200: Wakenyaku Co., Ltd., Kyoto, Japan).

Immunohistochemistry and Western blotting analysis

The protocol for immunohistochemical analysis was as previously described [12, 13]. Sirius red staining analysis was performed using a Picrosirius Red Stain Kit (Polysciences, St Louis, MO), according to the manufacturer's protocol. Tubular injury was evaluated in 10 periodic acid Schiff-stained sections. Evidence of tubular cell injury was scored on a semiquantitative scale from 0 to 3 for: i) loss of brush border; ii) epithelial cell vacuolization; iii) epithelial cell desquamation; and iv) tubular dilation. Results from each item were added to yield the tubular injury score, with a maximal value of 12 [15, 16]. The protocol for Western blotting analysis was as previously described [13]. Primary antibodies were as follows: anti-mixed lineage kinase domain-like (MLKL) antibody (#37705; Cell Signaling Technology, Danvers, MA), phosphorylated MLKL (P-MLKL) (#37333; Cell Signaling Technology), anti-tubulin antibody (C11; Santa Cruz Biotechnology, Dallas, TX), anti-megalin polyclonal antibody (ab76969; abcam,

Cambridge, MA), anti-megalin monoclonal antibody (SC515750; Santa Cruz Biotechnology), anti-3 nitrotyrosine (NT) antibody (ab61392; abcam), anti-ARG2 antibody (27987; Thermo Fisher Scientific, Waltham, MA), and anti-TRβ antibody (j51; Santa Cruz Biotechnology).

Quantitative real-time PCR

Total RNA (200 ng) was used in real-time PCR, as described previously [14]. Specific primers were purchased from Thermo Fisher Scientific.

Flow cytometric analysis

The protocols for flow cytometric analysis of mice kidneys were as previously described [13]. Cells were stained with fluorescently labeled anti-CD11b and anti-Ly6c (BD Biosciences, Franklin Lakes, NJ). Flow cytometric analyses for the population of inflammatory cells were performed using a FACSCelesta™ flow cytometer (BD Biosciences).

PTCs were sorted using a FACSaria II flow cytometer, according to the manufacturer's protocol (BD Biosciences). Anti-CD10 antibodies (Bioss Antibodies, Woburn, MA) and anti-CD13 antibodies (BD Biosciences) were used to recognize PTCs [13]. The protocols for sorting cells from mouse kidneys were as previously described [13].

Determination of ROS levels and ARG activity

ROS generation was measured by 20,70-dichlorofluorescein diacetate (DCFH-DA) fluorescence emission (Merck). DCFH-DA is membrane permeable and is rapidly oxidized to the highly fluorescent 2,7-dichlorofluorescein in the presence of intracellular ROS. Samples were excited at 488 nm, and emissions were collected using a 525-nm long-pass filter and expressed as nanomoles per milligram of protein. ARG activities in the kidney of mice were quantified using an Arginase activity assay kit (Cosmo Biotechnology, Tokyo, Japan).

Statistical analysis

Two-tailed Mann-Whitney *U* tests were used for comparisons between two groups (Figs. 1–6), and one-way analysis of variance followed by the Tukey post-test was used for comparisons of three or more groups (Figs. 5 and 6). All data analyses were performed using STATA version 14.2 (Stata Corp LLC, College Station, TX).

Results

To analyze the effect of hyperthyroidism on the kidney under I/R, mice treated with LT4 or vehicle were subjected to I/R. Serum T4 and T3 were significantly elevated in hyperthyroid mice compared with euthyroid mice (Fig. 1A and 1B). Levels of T4 and T3 did not differ significantly between sham and I/R mice. Body weight and systolic blood pressure levels likewise showed no significant differences between sham and I/R euthyroid and hyperthyroid mice (Fig. 1C and 1D). Serum blood urea nitrogen (BUN) levels were increased by I/R in euthyroid mice (Fig. 1E). In hyperthyroid mice, BUN levels were significantly increased by I/R and serum creatinine (Cr) levels were also significantly increased in mice with I/R, compared with sham mice (Fig. 1F). In euthyroid mice, no elevation of Cr was observed following 45 min of I/R.

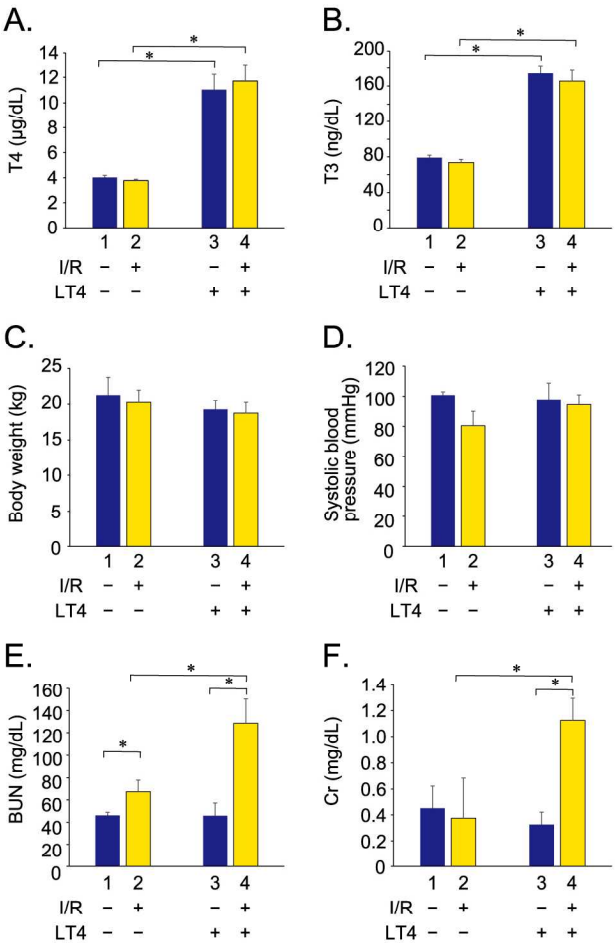

Fig. 1 Ischemic/reperfusion (I/R) injury is exacerbated by hyperthyroidism

Serum T4, T3, blood urea nitrogen (BUN), and creatinine (Cr) levels, and body weight (BW) are analyzed 14 days after I/R. Data are expressed as mean ± standard deviation (SD). $n = 9$, * $p < 0.05$. Experiments were performed in triplicate. LT4, L-thyroxine treatment.

Next, we examined kidney tissues by periodic acid-Schiff staining (Fig. 2A, a–d) and quantified tubular injury scores (Fig. 2B). After I/R injury, euthyroid mice showed destruction of the kidneys as indicated by the deterioration of tubular dilation (Fig. 2A, b, arrow 1). Hyperthyroid mice with I/R showed severe structural

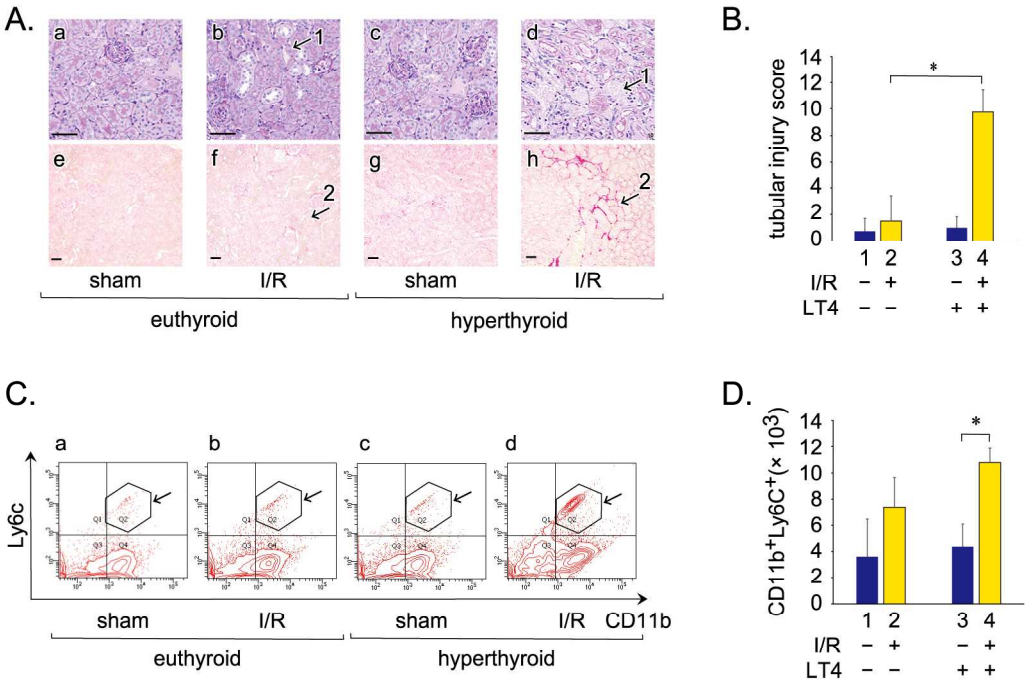

Fig. 2 Hyperthyroidism enhances tubular damage in the kidney with I/R

A) Representative photomicrographs of Periodic acid-Schiff staining (a–d) and Sirius red staining (e-h). Arrows labeled 1 indicate tubular cell lysis. Arrows labeled 2 indicate intestinal fibrosis. Scale bar: 50 μm. B) Tubular injury scores are calculated from 10 sections and expressed as mean ± SD. n = 10, * $p < 0.05$. C) Representative flow cytometric plots of monocytes in the whole kidney of euthyroid or hyperthyroid mice with or without I/R. Area within the frame indicates CD11b+ Ly6c+ cells. D) Fractions of CD11b+ Ly6c+ cells are counted and expressed as mean ± SD. n = 6. Experiments were performed in triplicate.

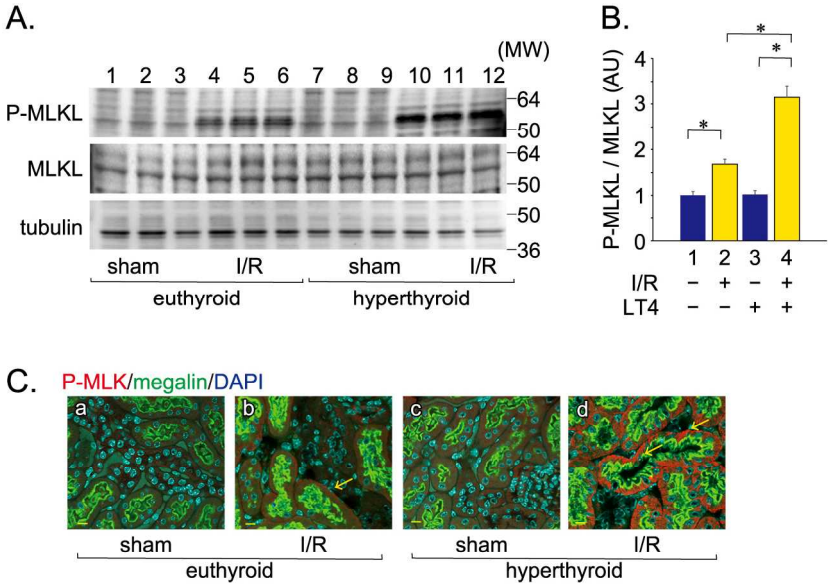

Fig. 3 Hyperthyroidism enhances tubular cell necroptosis in the kidney with I/R

A) Western blot analysis of expression levels of phosphorylated-MLKL (P-MLKL), MLKL, and tubulin in the kidney of euthyroid and hyperthyroid mice. B) Western blotting band intensities were quantified using Image J software and are presented as mean ± SD (error bars). n = 6, * $p < 0.05$. C) Expression of P-MLKL protein is detected using anti-P-MLKL antibody and Alexa Fluor 555-conjugated secondary antibody (red). Megalin expression is detected using anti-megalin antibody and Alexa Fluor 488-conjugated secondary antibody (green). Nuclei are stained with DAPI (blue). Arrows indicate protein expressions of P-MLKL in the membrane. Scale bar: 10 μm. All experiments were performed in triplicate.

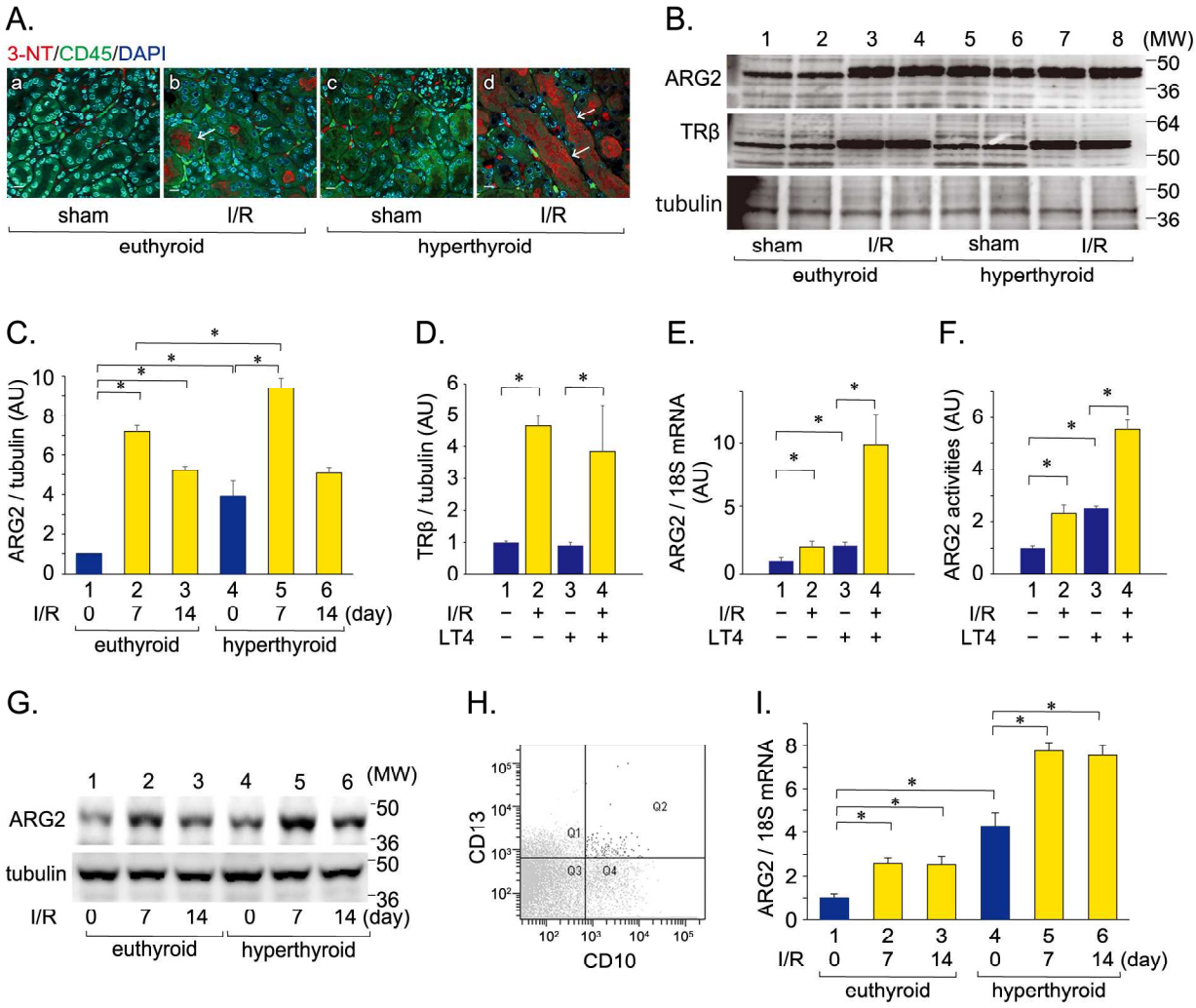

Fig. 4 I/R-induced arginase 2 expression is exacerbated by hyperthyroidism

A) Expression of 3-nitrotyrosine (3-NT) is detected using anti-3-NT antibody and Alexa Fluor 555-conjugated secondary antibody (red). CD45 expression is detected using anti-CD45 antibody and Alexa Fluor 488-conjugated secondary antibody (green). Nuclei are stained with DAPI (blue). Arrows indicate accumulation of 3-NT. Scale bar: 10 μm. B) Western blot analysis of expression levels of thyroid hormone receptor β (TRβ), arginase 2 (ARG2), and tubulin in the kidneys of euthyroid and hyperthyroid mice. C) D) Western blotting band intensities were quantified using Image J software and are presented as mean ± SD (error bars). AU, arbitrary units. $n = 9$, * $p < 0.05$. E) Levels of ARG2 mRNA are determined by quantitative real-time RT-PCR using 50 ng of cDNA. Relative quantification of ARG2 cDNA is performed by arbitrarily setting the control value from the sham-operated kidneys of euthyroid mice as 1. All data are expressed as mean ± SD (error bars). $n = 9$, * $p < 0.05$. F) Arginase activities in the kidneys of euthyroid or hyperthyroid mice. All data are expressed as mean ± SD (error bars). ARG2 activity is represented by arbitrarily setting the control value from the sham-operated kidneys of euthyroid mice as 1. $n = 9$, * $p < 0.05$. All experiments were performed in triplicate. G) Western blot analysis of expression levels of ARG2 and tubulin in the kidneys of euthyroid and hyperthyroid mice on days 0, 7, and 14 after I/R. H) Representative flow cytometric plots of proximal tubular cells in the whole kidney. Area of Q2 indicates $CD10^+$ $CD13^+$ cells. I) Levels of ARG2 mRNA are determined by quantitative real-time RT-PCR using 50 ng of cDNA of $CD10^+$ $CD13^+$ cells. Relative quantification of ARG2 cDNA is performed by arbitrarily setting the control value from the sham-operated kidneys of euthyroid mice at day 0 after I/R as 1.

destruction of the kidney with severe tubular lysis (Fig. 2A, d, arrow 1). At 14 days after I/R injury, renal interstitial fibrosis was mild (Fig. 2A, f, arrow 2) in euthyroid mice. Renal interstitial fibrosis tended to be increased in hyperthyroid mice after I/R injury (Fig. 2A, h, arrow 2), compared with euthyroid mice after I/R injury (Fig. 2A, f, arrow 2).

Like other organs, inflammatory cells are recruited to the kidney after severe I/R injury [17]. Macrophages are known to consist of subsets with varying cell surface markers, chemokine receptors and roles in injury and repair *versus* fibrosis. Mature monocytes expressing both CD11b and Ly6c infiltrate tissues and are implicated in disease processes. These cells have been

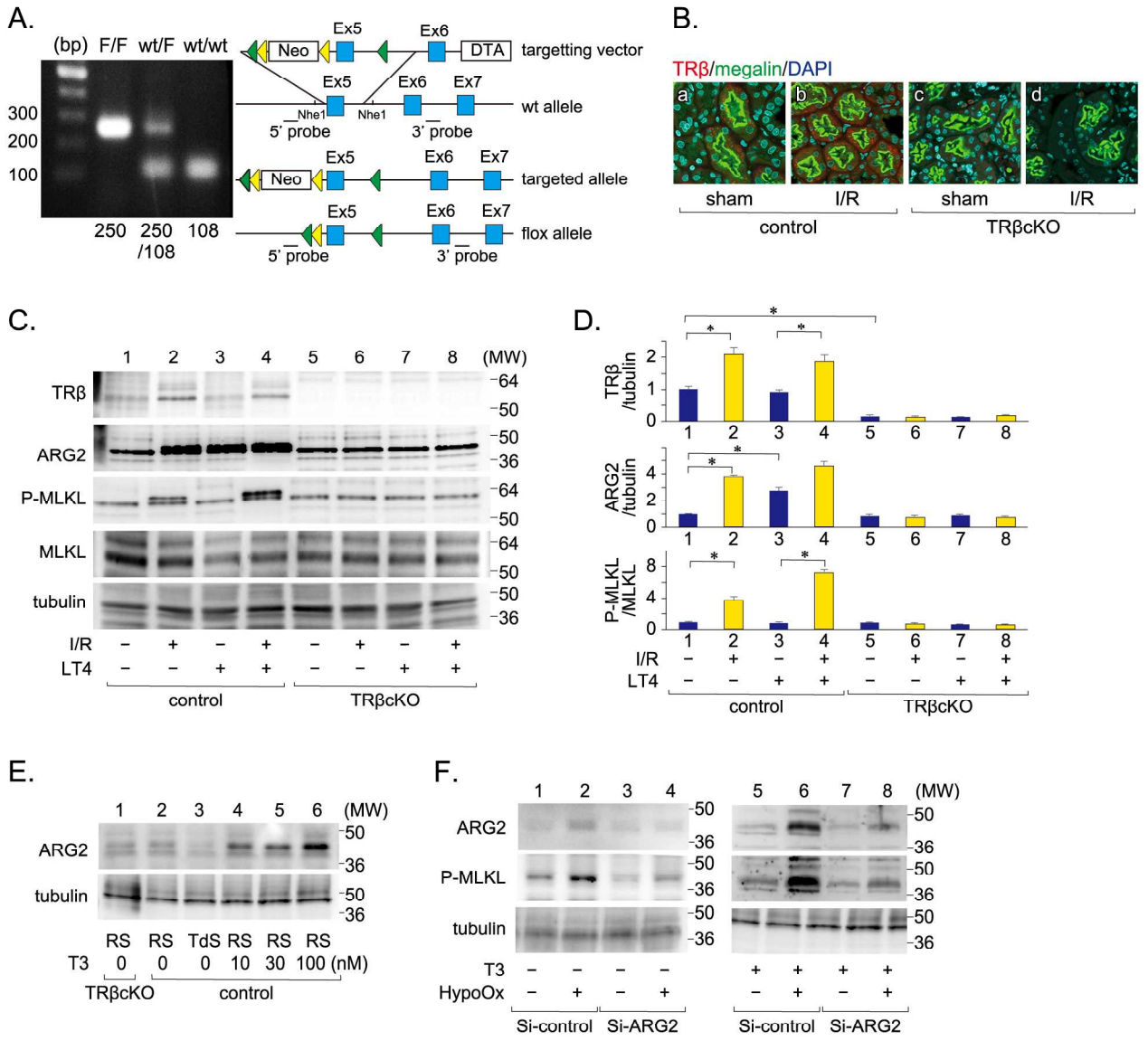

Fig. 5 Hyperthyroidism-induced ARG2 expression is inhibited in the kidneys of proximal tubular cell (PTC)-specific TRβ-knockout mice

A) TRβ allele used for Cre-mediated TRβ inactivation. Neo cassette flanked by 2 flippase recognition target (Frt) sites (△) is excised by flippase to create floxed allele. DTA indicates diphtheria toxin-A used to select against nonhomologous recombinants. Exons 5 and 6 (■) flanked by 2 LoxP sites (▲) are excised by Cre recombinase to create a null allele. The 5' probe and 3' probe indicate forward and reverse PCR primers used for genotyping, respectively. PCR products of tail genomic DNA of TRβ flox/flox (F/F) mice. Homozygous: 250 bp; heterozygous: 250/108 bp; and wild-type: 108 bp. B) a. Expression of TRβ is detected using anti-TRβ antibody and Alexa Fluor 555-conjugated secondary antibody (red). Megalin expression is detected using anti-megalin antibody and Alexa Fluor 488-conjugated secondary antibody (green). Nuclei are stained with DAPI (blue). Scale bar: 10 μm. C) Western blot analysis of expression levels of TRβ, ARG2, P-MLKL, MLKL, and tubulin in the kidney of control and PTC-specific TRβ-knockout mice (TRβcKO). D) Western blotting band intensities were quantified using Image J software and are presented as mean ± SD (error bars). $n = 9$, * $p < 0.05$. E) Western blot analysis of expression levels of ARG2 and tubulin in the primary cells of control or TRβcKO. RS, regular serum; TdS, T3-depleted medium. F) The effect of siRNA-knockdown of the ARG2 (or control siRNA) on the level of P-MLKL expression was analyzed using Western blotting. All experiments were performed in triplicate.

termed "inflammatory macrophages" [18]. Flow cytometric analysis indicated that I/R injury enhanced the accumulation of $CD11b^+$ and $Ly6c^+$ cells in the kidneys of euthyroid mice (Fig. 2C, a *vs.* b; Fig. 2D lane 1 *vs.* 2). In the kidneys of hyperthyroid mice, $CD11b^+$ and $Ly6c^+$ monocytes showed significant accumulation after I/R injury (Fig. 2C, c *vs.* d; Fig. 2D lane 3 *vs.* 4). These results supported the hypothesis that hyperthyroidism exacerbated I/R injury and caused severe structural destruction in the kidney.

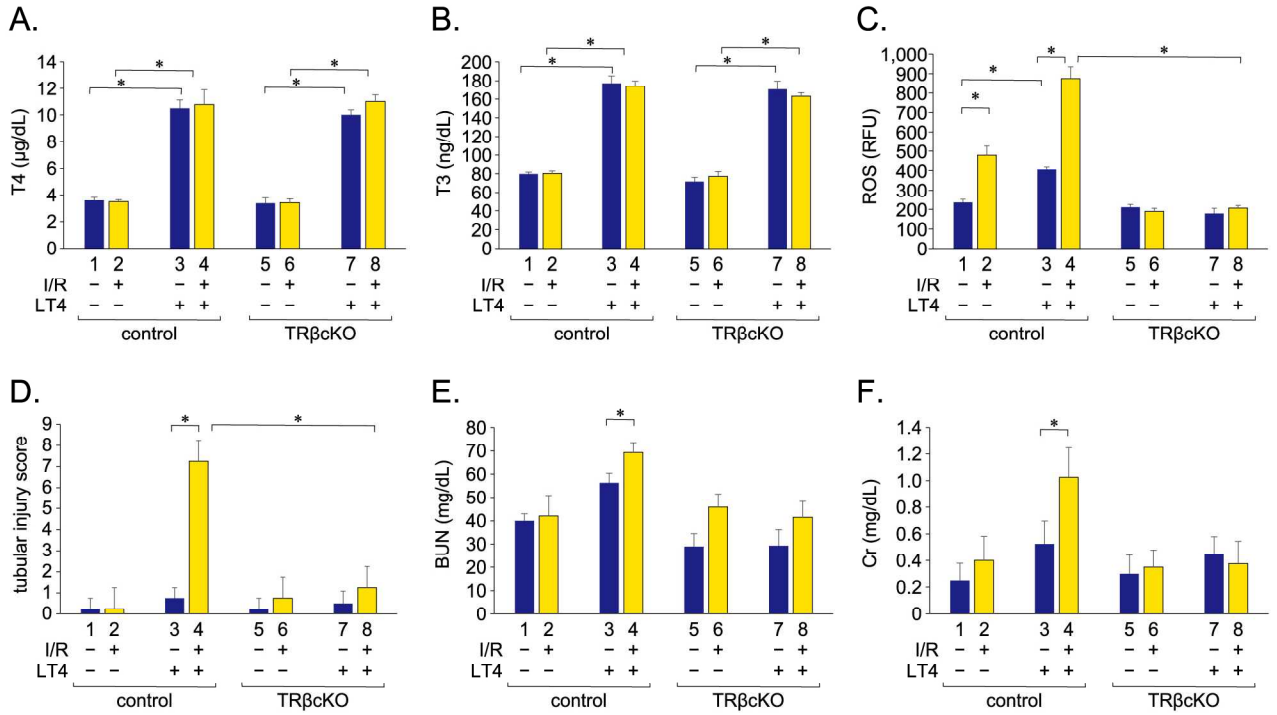

Fig. 6 Hyperthyroidism-enhanced kidney injury is ameliorated in the kidney of TRβcKO mice with I/R

Serum T4, T3, BUN, Cr levels, and tubular injury score and reactive oxygen species (ROS) of the kidney are expressed as mean ± SD. * $p < 0.05$, $n = 9$ All experiments were performed in triplicate.

To assess the cell injury process underlying hyperthyroid-induced kidney injury, we performed Western blotting analysis in triplicate for the expression of MLKL, a marker of necroptosis in the kidney (Fig. 3A and 3B). Phosphorylation of MLKL was enhanced in the kidneys of euthyroid mice subjected to I/R, as compared to sham mice (Fig. 3B). In hyperthyroid mice, I/R injury significantly enhanced the phosphorylation of MLKL, showing higher expression than euthyroid mice with I/R. Total MLKL expressions did not differ significantly between kidneys of euthyroid or hyperthyroid mice with or without I/R. Immunohistochemical analyses indicated the cellular distribution of P-MLKL in the kidneys (Fig. 3C). Megalin is a marker of PTCs [19]. P-MLKL protein expression was not observed in kidneys without I/R injury (Fig. 3C, a and c), while I/R injury enhanced the expression of P-MLKL protein in the cell membrane of PTCs that expressed megalin (Fig. 3C, b and d; arrows).

Three-nitrotyrosine (3-NT) is one of the main proteins nitrated by peroxynitrite and is used as a nitrosative stress marker [20]. Immunohistochemical analysis indicated that accumulation of 3-NT was enhanced in the renal tubular cells of euthyroid mice after I/R (Fig. 4A, b; arrow). Leukocytes identified as CD45-positive were accumulated around 3-NT-expressing tubular cells. In hyperthyroid mice, I/R induced higher amounts of 3-NT- and CD45-positive leucocytes accumulation in the cytosol of renal tubular cells, compared with euthyroid mice after I/R (Fig. 4A, d; arrows).

ARG is one of the targets of thyroid hormone signaling [2]. Recent reports have indicated that ARG2 is enhanced by I/R injury and plays a pivotal role in I/R-induced renal injury [6, 21]. ARG2 inhibitors were thus expected to provide effective treatment for I/R injury [6, 21]. ARG2 protein expression was enhanced in the kidneys of euthyroid mice at 14 days after I/R (Fig. 4B and 4C). ARG2 expression was enhanced in the kidneys of hyperthyroid mice, compared with euthyroid mice. The temporal changes in ARG2 expression in the kidney after I/R in euthyroid and hyperthyroid mice are shown in Fig. 4G. I/R injury significantly enhanced ARG2 expression in the kidneys of hyperthyroid mice, compared with euthyroid mice, at 7 days after I/R (Fig. 4C and 4G). ARG2 induction was maximally elevated at 7 days after I/R and decreased at 14 days after I/R. TRβ protein expression was enhanced by I/R in the kidneys of euthyroid and hyperthyroid mice at 14 days after I/R (Fig. 4B and 4D). ARG2 mRNA expression was enhanced in the kidneys of hyperthyroid mice, compared with euthyroid mice (Fig. 4E). I/R injury significantly enhanced the mRNA expression of ARG2 in the kidneys of hyperthyroid mice at 14 days after I/R. To clarify the distribution of ARG2 in the kidney, PTCs were co-labeled with anti-CD10 antibodies and anti-CD13 antibodies (Fig. 4H Q2)

and collected using the cell-sorter. Expression of ARG2 mRNA was significantly enhanced in PTCs from the kidneys of euthyroid mice that underwent I/R after both 7 and 14 days (Fig. 4I). Hyperthyroidism additively enhanced the ARG2 mRNA expression in the PTCs of I/R-injured mice. ARG2 enzyme activities were enhanced in the kidneys of hyperthyroid mice, compared with euthyroid mice (Fig. 4F). I/R injury significantly enhanced ARG2 activities in the kidneys of both euthyroid and hyperthyroid mice at 14 days after I/R. These results suggested that I/R injury induced expression of ARG2, with this induction exacerbated by hyperthyroidism for PTCs in the kidney.

To analyze the molecular mechanisms of ARG2 induced by I/R and hyperthyroidism, we generated conditional knockout mice with PTC-specific inhibition of TRβ expression (TRβcKO) (Fig. 5A). TRβcKO mice were generated by crossing $TR\beta^{F/F}$ with knock-in mice harboring Tam-inducible Cre-recombinase gene driven by a PTC-specific Ndrg1 promoter [10]. Immunohistochemical analysis indicated that endogenous TRβ expression was abundantly expressed in PTCs that expressed megalin (Fig. 5B, a). With Tam-treatment, TRβ expression was significantly decreased in the PTCs of TRβcKO mice, confirming that TRβ-inactivation by the Cre-loxP system was effective in TRβcKO mice (Fig. 5B, a *vs.* c; C).

TRβcKO mice and control mice (TRβcKO mice without Tam-administration) were treated with LT4 or vehicles and operated on to create I/R injury. As with data from wild-type mice (Fig. 4), ARG2 expression was enhanced after I/R and exacerbated under hyperthyroidism (Fig. 5C and 5D) in control mice. In TRβcKO mice, such I/R-induced ARG2 induction was not observed (lanes 5–8). Phosphorylation of MLKL was enhanced by I/R injury under hyperthyroidism, while P-MLKL-induction was not observed in the kidneys of TRβcKO mice.

To analyze the association of induction of ARG2 and PTC-injury, primary culture cells were isolated from the kidneys of wild control or TRβcKO mice. Expression of ARG2 did not differ significantly between the primary cells of control and TRβcKO mice (Fig. 5E), while ARG2 expression was decreased in those cells cultured with TdS-containing medium. Ten, 30, or 100 nM of T3 treatment enhanced the expression of ARG2 in a dose-dependent manner. These results are consistent with previous findings [22] that ARG2 transcription was regulated by TRβ as a ligand-dependent transcription factor and repressed by unliganded-TRβ in basal transcriptional suppression.

We also analyzed the effects of ARG2-downregulation on hypoxia-induced cell necroptosis of PTCs using ARG2-specific siRNA. Primary cells were transfected with either control or ARG2 siRNA and were then incubated for 48 h. Primary cultured cells were subsequently treated with or without 300 nM of T3-treatment, following incubation under normoxia or hypoxia for an additional 12 h. Hypoxia enhanced the expressions of ARG2 and P-MLKL (Fig. 5F). Hypoxia-induced ARG2 expression was completely inhibited in ARG2 siRNA-transfected cells and MLKL phosphorylation was decreased. Hypoxia and T3-treatment exacerbated the expression of ARG2 and MLKL phosphorylation, while induction of ARG2 and P-MLKL was completely inhibited in ARG2 siRNA-transfected cells. These *in vitro* studies suggested that hypoxia and excess thyroid hormone-induced cell necroptosis are involved in the induction of ARG2.

In hyperthyroid mice, serum T4 and T3 levels were significantly increased compared with euthyroid mice (Fig. 6A and 6B, respectively). ROS levels in the kidney were quantified by analyzing fluorescence intensities. ROS levels were increased by I/R injury (Fig. 6C, lane 2 *vs.* 1). Hyperthyroid condition increased ROS accumulation in the kidney (Fig. 6C, lane 3 *vs.* 1), and I/R enhanced ROS accumulation in the kidney under hyperthyroid conditions (lane 4 *vs.* 3). Otherwise, ROS elevation was not observed in the kidney of TRβcKO mice (lanes 5–6). I/R enhanced tubular injuries in the kidneys of hyperthyroid mice (Fig. 6D, line 3), accompanied by elevation of BUN and Cr (Fig. 6E, line 3 and 6F line 3, respectively). These kidney injuries were ameliorated by inhibition of the thyroid hormone signal in TRβcKO mice (lanes 5–6). I/R-induced pathological changes were also ameliorated in the kidneys of TRβcKO mice (data not shown). These results indicate that inhibition of excess thyroid hormone signals reduced ARG2 and ROS, and ameliorated kidney injury after I/R.

Discussion

This study analyzed the effects of hyperthyroidism on I/R injury. Excess thyroid hormone enhanced expression of ARG2, which induced accumulation of ROS and necroptosis of PTCs and exacerbated the kidney injury. PTC-specific knockdown of TRβ and its signals could ameliorate I/R injury, *via* inhibition of I/R-induced ARG2-induction.

Fig. 1 and 2 demonstrate that the damage from 45 min of I/R is tolerable by the kidneys of euthyroid mice, whereas 45 min of I/R in the kidneys of hyperthyroid mice induced severe kidney injury, fibrosis, and dysfunction. Blood pressure and body weight did not differ significantly between euthyroid and hyperthyroid mice. Pathological findings indicated that severe damage to

PTCs was observed in the kidneys of hyperthyroid mice. I/R injury induced the phosphorylation of MLKL and membrane translocation, which was enhanced under hyperthyroid conditions. These results indicate that I/R injury-induced cell necroptosis was exacerbated by hyperthyroidism. Fig. 4 indicates that inflammatory monocytes accumulated in the interstitial space around necroptotic PTCs. Such results suggest that non-infectious inflammation was initiated in the I/R-injured kidneys of hyperthyroid mice.

To explore the molecular mechanisms underlying excess thyroid hormone exacerbating I/R injury in the kidney, we focused on I/R-induced accumulation of 3-NT and upregulation of ARG2 in PTCs. ARG2 expression and activities were significantly decreased in the kidneys of TRβcKO mice subjected to I/R (Fig. 4). The L-arginine-ROS pathway plays a pivotal role in the management of I/R injury [6]. Direct data on the relationship between thyroid hormones, ARG2, and ROS remain lacking. Excessive ARG2 activity increased levels of ornithine and proline, which contribute to pathological fibrosis. ARG expression is regulated by thyroid hormone signals during amphibian metamorphosis in *Xenopus laevis* [23], while our study is the first report of analyses using I/R-injured mice. ARG2 expression levels in the kidney were maximally increased at day 7 after I/R in hyperthyroid mice and remained elevated at day 14 after I/R. Hyperthyroidism exacerbated the I/R injury of the kidney. Our study indicated that excess thyroid hormones are disadvantageous for I/R-injured kidneys, and are involved in the induction of ARG2 in PTCs. Overt hypothyroidism represents a state of severe thyroid hormone deficiency that requires LT4 treatment. In contrast, whether subclinical hypothyroidism should be treated remains controversial, as overreplacement or iatrogenic thyrotoxicosis are associated with increased cardiovascular risk [24, 25].

The most important mechanisms by which AKI develops to CKD are tubular epithelial cell loss and intestinal fibrosis [22]. Renal I/R injury is a common cause of AKI and is involved in impairment of oxygen and nutrient delivery, and reduced removal of waste products from the kidney. Imbalances in tissue oxygen supply and demand and the accumulation of waste products enhance the injury to tubular cells. If severe, cell death occurs by necroptosis. During the recovery process of AKI, tubular cell death is followed by tubular differentiation, proliferation, and regeneration, accompanied by inflammation [26]. A recent study indicated that regulated necrosis pathways such as necroptosis and ferroptosis play key roles in AKI [27]. Necroptosis involves the formation of the necroptosome, a necroptosis-inducing complex that phosphorylates MLKL [26]. Phosphorylation of MLKL triggers its membrane translocation, followed by the initiation of necrosis. Cell death through necrosis, necroptosis, or ferroptosis results in the release of intracellular organelles and inflammatory damage-associated molecular patterns that potentiate the inflammatory response, recruiting inflammatory cells [28].

Our study demonstrated for the first time that ligand-bound-TR plays an essential role in the progression of cell death and fibrosis. By targeting ARG2 expressed in PTCs, ligand-bound TR is involved in the expression of P-MLKL and 3-NT. A better understanding of the molecular and genetic aspects of kidney injury will facilitate the design of more targeted therapies to prevent injury and hasten repair.

Acknowledgments

None.

Author Disclosure Statement

There are no conflicts to disclose.

References

1. Lazar MA (1993) Thyroid hormone receptors: multiple forms, multiple possibilities. *Endocr Rev* 14: 184–193.
2. Rodriguez-Gomez I, Moliz JN, Quesada A, Montoro-Molina S, Vargas-Tendero P, *et al.* (2016) L-Arginine metabolism in cardiovascular and renal tissue from hyper- and hypothyroid rats. *Exp Biol Med (Maywood)* 241: 550–556.
3. Iglesias P, Bajo MA, Selgas R, Diez JJ (2017) Thyroid dysfunction and kidney disease: an update. *Rev Endocr Metab Disord* 18: 131–144.
4. Rodriguez-Gomez I, Manuel Moreno J, Jimenez R, Quesada A, Montoro-Molina S, *et al.* (2015) Effects of arginase inhibition in hypertensive hyperthyroid rats. *Am J Hypertens* 28: 1464–1472.
5. Wu G, Morris SM Jr (1998) Arginine metabolism: nitric oxide and beyond. *Biochem J* 336: 1–17.
6. Hara M, Torisu K, Tomita K, Kawai Y, Tsuruya K, *et al.* (2020) Arginase 2 is a mediator of ischemia-reperfusion injury in the kidney through regulation of nitrosative stress. *Kidney Int* 98: 673–685.
7. Basile DP, Anderson MD, Sutton TA (2012) Pathophysiology of acute kidney injury. *Compr Physiol* 2: 1303–

1353.
8. Lameire NH, Bagga A, Cruz D, De Maeseneer J, Endre Z, *et al.* (2013) Acute kidney injury: an increasing global concern. *Lancet* 382: 170–179.
9. Caldwell RW, Rodriguez PC, Toque HA, Narayanan SP, Caldwell RB (2018) Arginase: a multifaceted enzyme important in health and disease. *Physiol Rev* 98: 641–665.
10. Endo T, Nakamura J, Sato Y, Asada M, Yamada R, *et al.* (2015) Exploring the origin and limitations of kidney regeneration. *J Pathol* 236: 251–263.
11. Okuda T, Higashi Y, Kokame K, Tanaka C, Kondoh H, *et al.* (2004) Ndrg1-deficient mice exhibit a progressive demyelinating disorder of peripheral nerves. *Mol Cell Biol* 24: 3949–3956.
12. Ishii T, Furuya F, Takahashi K, Shikata M, Takamura T, *et al.* (2019) Angiopoietin-like protein 2 promotes the progression of diabetic kidney disease. *J Clin Endocrinol Metab* 104: 172–180.
13. Furuya F, Ishii T, Tamura S, Takahashi K, Kobayashi H, *et al.* (2017) The ligand-bound thyroid hormone receptor in macrophages ameliorates kidney injury *via* inhibition of nuclear factor-κB activities. *Sci Rep* 7: 43960.
14. Ichijo S, Furuya F, Shimura H, Hayashi Y, Takahashi K, *et al.* (2014) Activation of the RhoB signaling pathway by thyroid hormone receptor β in thyroid cancer cells. *PLoS One* 9: e116252.
15. Moreno JA, Izquierdo MC, Sanchez-Nino MD, Suarez-Alvarez B, Lopez-Larrea C, *et al.* (2011) The inflammatory cytokines TWEAK and TNFα reduce renal klotho expression through NFκB. *J Am Soc Nephrol* 22: 1315–1325.
16. Martin-Sanchez D, Ruiz-Andres O, Poveda J, Carrasco S, Cannata-Ortiz P, *et al.* (2017) Ferroptosis, but not necroptosis, is important in nephrotoxic folic acid-induced AKI. *J Am Soc Nephrol* 28: 218–229.
17. Jang HR, Rabb H (2015) Immune cells in experimental acute kidney injury. *Nat Rev Nephrol* 11: 88–101.
18. Jurewicz M, McDermott DH, Sechler JM, Tinckam K, Takakura A, *et al.* (2007) Human T and natural killer cells possess a functional renin-angiotensin system: further mechanisms of angiotensin II-induced inflammation. *J Am Soc Nephrol* 18: 1093–1102.
19. Nielsen R, Christensen EI, Birn H (2016) Megalin and cubilin in proximal tubule protein reabsorption: from experimental models to human disease. *Kidney Int* 89: 58–67.
20. Teerlink T, Nijveldt RJ, de Jong S, van Leeuwen PA (2002) Determination of arginine, asymmetric dimethylarginine, and symmetric dimethylarginine in human plasma and other biological samples by high-performance liquid chromatography. *Anal Biochem* 303: 131–137.
21. Kim JH, Bugaj LJ, Oh YJ, Bivalacqua TJ, Ryoo S, *et al.* (2009) Arginase inhibition restores NOS coupling and reverses endothelial dysfunction and vascular stiffness in old rats. *J Appl Physiol* (1985) 107: 1249–1257.
22. Chawla LS, Amdur RL, Amodeo S, Kimmel PL, Palant CE (2011) The severity of acute kidney injury predicts progression to chronic kidney disease. *Kidney Int* 79: 1361–1369.
23. Patterton D, Shi YB (1994) Thyroid hormone-dependent differential regulation of multiple arginase genes during amphibian metamorphosis. *J Biol Chem* 269: 25328–25334.
24. Teumer A, Chaker L, Groeneweg S, Li Y, Di Munno C, *et al.* (2018) Genome-wide analyses identify a role for SLC17A4 and AADAT in thyroid hormone regulation. *Nat Commun* 9: 4455.
25. Biondi B, Cooper DS (2019) Thyroid hormone therapy for hypothyroidism. *Endocrine* 66: 18–26.
26. Vanden Berghe T, Linkermann A, Jouan-Lanhouet S, Walczak H, Vandenabeele P (2014) Regulated necrosis: the expanding network of non-apoptotic cell death pathways. *Nat Rev Mol Cell Biol* 15: 135–147.
27. Bonventre JV, Yang L (2011) Cellular pathophysiology of ischemic acute kidney injury. *J Clin Invest* 121: 4210–4221.
28. Jansen MP, Emal D, Teske GJ, Dessing MC, Florquin S, *et al.* (2017) Release of extracellular DNA influences renal ischemia reperfusion injury by platelet activation and formation of neutrophil extracellular traps. *Kidney Int* 91: 352–364.